

Critical Investigation of Defect Site Functionalization on Single-Walled Carbon Nanotubes

Elisa Del Canto,[‡] Kevin Flavin,[‡] Dania Movia,[‡] Cristina Navio,[§] Carla Bittencourt,[§] and Silvia Giordani^{*‡}

[‡]School of Chemistry/Centre for Research on Adaptive Nanostructures and Nanodevices (CRANN), University of Dublin, Trinity College, Dublin 2, Ireland, and [§]University of Mons, Parc Initialis, Av. Nicolas Copernic 1, Mons 7000, Belgium

Received July 16, 2010. Revised Manuscript Received November 23, 2010

The presence of carboxylated carbonaceous material in nitric acid-treated single-walled carbon nanotube (SWNT) samples has recently brought renewed focus on the processes by which covalent functionalization of such materials are carried out. Using a widely reported 2-step purification/oxidation procedure, we have investigated the effect of basic treatment and solvent washing on the functionalization and final properties and behavior of SWNTs. We have demonstrated, using a number of spectroscopic techniques, that in the absence of NaOH treatment, COOH functionality is introduced directly onto SWNTs, and not only onto carbonaceous material present in the sample. Covalent functionalization of the oxidized materials was also investigated by attachment of a fluorescent probe, and ultimately, whether treated with base or solvent washed, the resulting materials are close to identical with respect to both their appearance and properties. In addition, we have demonstrated that using either of these purification/oxidation strategies, functionalized materials can be produced that still exhibit distinctive optical/electronic properties, as demonstrated by sustained structured spectroscopic absorption and emission features.

Introduction

Single-walled carbon nanotubes (SWNTs)^{1,2} are a unique class of material that have received an enormous amount of attention over recent years, because of their remarkable mechanical,³ thermal,⁴ electronic,^{5,6} and optical^{7,8} properties. However, a number of practical aspects such as purity, solubility and processability still impede their widespread exploitation. Great effort has recently been exerted with regards to their chemical treatment and functionalization to overcome these problems and also to drive toward the production of more manageable multifunctional materials.

Two approaches have been widely reported in the literature for the chemical modification of SWNTs, which involve either the noncovalent adsorption onto the

nanotube surface^{9,10} or the covalent attachment to the π -conjugated skeleton.^{11,12} There are obvious advantages related to the covalent strategy, such as control over the number of functional moieties that may be attached,^{13–15} in addition to the well-defined nature and stability of the linker that connects them to the nanotube. Care must be taken however, as the optical, electronic and thermal properties depend heavily upon the highly conjugated form in which the SWNTs exist,^{6,16,17} and their covalent modification, depending on its location, can result in loss of those properties.¹⁸

Two general strategies exist for covalently attaching functional molecules to the nanotube structure. The first involves reaction of a reagent or functional molecule at the sidewall of the tube and has been performed using nucleophilic-, electrophilic-, radical-, and cycloaddition based mechanistic approaches.¹⁹ Introduction of a covalent

*To whom correspondence should be addressed. E-mail: giordans@tcd.ie.

- (1) Iijima, S. *Nature* **1991**, *354*, 56–58.
- (2) Iijima, S.; Ichihashi, T. *Nature* **1993**, *363*, 603–605.
- (3) Treacy, M. M. J.; Ebbesen, T. W.; Gibson, J. M. *Nature* **1996**, *381*, 678–680.
- (4) Berber, S.; Kwon, Y. K.; Tomanek, D. *Phys. Rev. Lett.* **2000**, *84*, 4613–4616.
- (5) Mintmire, J. W.; Dunlap, B. I.; White, C. T. *Phys. Rev. Lett.* **1992**, *68*, 631–634.
- (6) Itkis, M. E.; Niyogi, S.; Meng, M. E.; Hamon, M. A.; Hu, H.; Haddon, R. C. *Nano Lett.* **2002**, *2*, 155–159.
- (7) Kataura, H.; Kumazawa, Y.; Maniwa, Y.; Umez, I.; Suzuki, S.; Ohtsuka, Y.; Achiba, Y. *Synth. Met.* **1999**, *103*, 2555–2558.
- (8) Hasan, T.; Sun, Z. P.; Wang, F. Q.; Bonaccorso, F.; Tan, P. H.; Rozhin, A. G.; Ferrari, A. C. *Adv. Mater.* **2009**, *21*, 3874–3899.
- (9) Chen, R. J.; Zhang, Y.; Wang, D.; Dai, H. J. *Am. Chem. Soc.* **2001**, *123*, 3838–3839.
- (10) Britz, D. A.; Khlobystov, A. N. *Chem. Soc. Rev.* **2006**, *35*, 637–659.

- (11) Banerjee, S.; Hemraj-Benny, T.; Wong, S. S. *Adv. Mater.* **2005**, *17*, 17–29.
- (12) Singh, P.; Campidelli, S.; Giordani, S.; Bonifazi, D.; Bianco, A.; Prato, M. *Chem. Soc. Rev.* **2009**, *38*, 2214–2230.
- (13) Prato, M. *Nature* **2010**, *465*, 172–173.
- (14) Syrgiannis, Z.; Gebhardt, B.; Dotzer, C.; Hauke, F.; Graupner, R.; Hirsch, A. *Angew. Chem., Int. Ed.* **2010**, *49*, 3322–3325.
- (15) Voiry, D.; Roubeau, O.; Penicaud, A. *J. Mater. Chem.* **2010**, *20*, 4385–4391.
- (16) Niyogi, S.; Hamon, M. A.; Hu, H.; Zhao, B.; Bhowmik, P.; Sen, R.; Itkis, M. E.; Haddon, R. C. *Acc. Chem. Res.* **2002**, *35*, 1105–1113.
- (17) Burghard, M. *Surf. Sci. Rep.* **2005**, *58*, 1–109.
- (18) Strano, M. S.; Dyke, C. A.; Usrey, M. L.; Barone, P. W.; Allen, M. J.; Shan, H. W.; Kittrell, C.; Hauge, R. H.; Tour, J. M.; Smalley, R. E. *Science* **2003**, *301*, 1519–1522.
- (19) Tasis, D.; Tagmatarchis, N.; Bianco, A.; Prato, M. *Chem. Rev.* **2006**, *106*, 1105–1136.

bond at the sidewall, however, inherently results in loss of the sp^2 character of the reacting carbon and thus also in a break in conjugation at that point on the tube. This, depending on the number of functional groups attached, can result in complete loss of characteristic electronic and optical properties.¹⁸ The second strategy has been widely used and involves the addition of functional moieties to oxidized defect sites produced during acidic/oxidative purification of the nanotubes. Nitric acid has been used as a standard reagent in an attempt to remove synthetic byproducts, such as residual catalyst particles and amorphous carbon, from raw SWNT samples.^{20–24} It has been shown that depending on both the time of reaction and the nitric acid concentration, the purification procedure may introduce varying numbers of oxygenated functionalities (mainly carbonyl and carboxylic acid groups) onto defect sites, to which further functionality may be subsequently attached.²³

It has recently been reported that small polycyclic aromatic sheets edge-terminated with carboxyl groups, coined as carboxylated carbonaceous fragments (CCFs), are also generated during the acidic/oxidative purification procedure and it is understood that they form a “uniform and reactive coating on the SWNTs”.^{22,25,26} The effective removal of the CCFs from acid purified samples by NaOH treatment has been demonstrated,^{26–28} and it has therefore come into contention as to whether reactions carried out, following the purification step, actually result in covalent modification of the nanotubes or only result in functionalization of the CCFs. Haddon and co-workers have more recently shown that nitric acid purified samples exhaustively washed with aqueous base nevertheless contained a sufficient number of carboxylic acid groups to prepare high quality covalently functionalized nanotubes.²⁹

These recent studies raise some important questions as to whether previously reported procedures presenting

covalent functionalization using defect site chemistry,^{30–34} in the absence of NaOH treatment, were actually producing covalently functionalized materials, and also how the final properties of the functionalized materials are affected by the presence or absence of NaOH treatment. To attempt to answer these questions, oxidized SWNTs were prepared in two batches using a widely reported 2-step purification/oxidation procedure,^{19,35–38} comparable to the one initially developed by Smalley and co-workers.^{39,40} The first batch was subjected to the NaOH treatment reported by Green and co-workers,²⁶ and the second batch was washed with a number of solvents. A fluorescent label was subsequently attached to each batch as a simple method of monitoring functionalization, and using a variety of complementary characterization techniques, we have demonstrated that with or without NaOH treatment, once materials are thoroughly washed, the functionalized SWNTs that are produced are nearly identical. We have also shown that both procedures are capable of producing covalently functionalized SWNTs that still display structured emission and absorption features indicating preservation of their electronic properties.

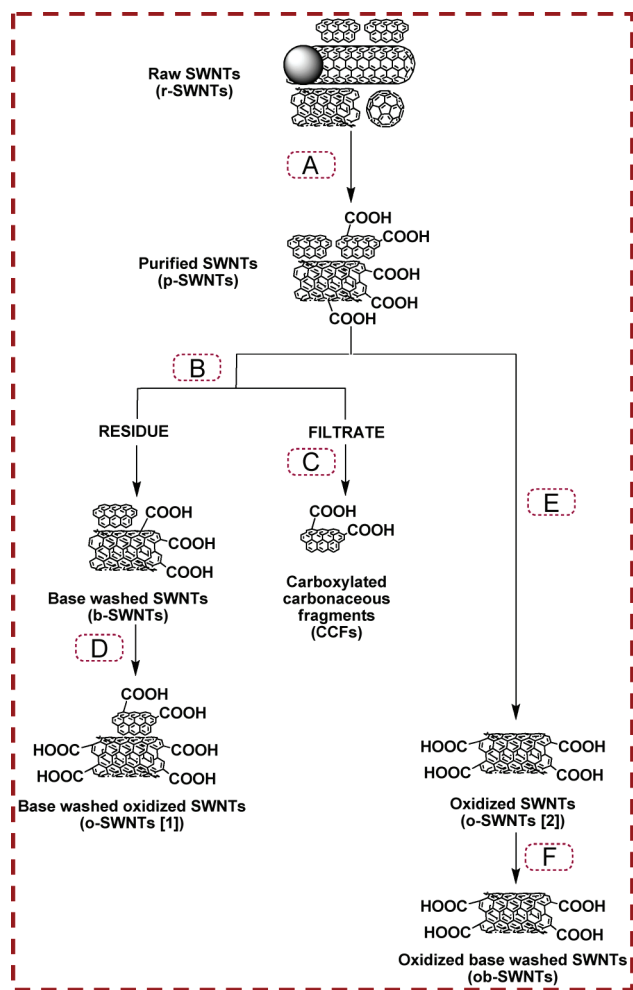
Results and Discussion

Purification/Oxidation. The purification of as purchased raw SWNTs was performed using a widely reported protocol, which consists of refluxing the nanotubes in an aqueous dispersion of nitric acid for 48 h (Scheme 1).³⁹ The strong acidic conditions are used to remove catalytic iron nanoparticles and also to oxidize defect sites on the SWNTs, with carboxylated carbonaceous fragments (CCFs) being produced as a byproduct. The purified sample (p-SWNTs) was split into two batches, of which the first was subjected to the NaOH treatment to produce b-SWNTs and the second was sonicated in organic solvents followed by filtration. Thereafter both batches were further oxidized for 1 h at 35 °C in a mixture of sulphuric acid and hydrogen peroxide to produce o-SWNTs **1** and **2**. Following each synthetic step, it was ensured that the nanotubes were washed thoroughly with water until a neutral pH was reached, and subsequently dispersed in DMF by sonication and washed with DMF and methanol until the filtrate ran clear (Scheme 1). The washing procedures and the filtrate pictures are reported in the Supporting Information (Scheme S1).

- (20) Haddon, R. C. *Science* **1993**, *261*, 1545–1550.
 (21) Tohji, K.; Goto, T.; Takahashi, H.; Shinoda, Y.; Shimizu, N.; Jayadevan, B.; Matsuoka, I.; Saito, Y.; Kasuya, A.; Ohsuna, T.; Hiraga, H.; Nishina, Y. *Nature* **1996**, *383*, 679.
 (22) Dillon, A. C.; Gennett, T.; Jones, K. M.; Alleman, J. L.; Parilla, P. A.; Heben, M. J. *Adv. Mater.* **1999**, *11*, 1354–1358.
 (23) Hu, H.; Zhao, B.; Itkis, M. E.; Haddon, R. C. *J. Phys. Chem. B* **2003**, *107*, 13838–13842.
 (24) Giordani, S.; Colomer, J. F.; Cattaruzza, F.; Alfonsi, J.; Meneghetti, M.; Prato, M.; Bonifazi, D. *Carbon* **2009**, *47*, 578–588.
 (25) Rinzler, A. G.; Liu, J.; Dai, H.; Nikolaev, P.; Huffman, C. B.; Rodriguez-Macias, F. J.; Boul, P. J.; Lu, A. H.; Heymann, D.; Colbert, D. T.; Lee, R. S.; Fischer, J. E.; Rao, A. M.; Eklund, P. C.; Smalley, R. E. *Appl. Phys. A: Mater. Sci. Process.* **1998**, *67*, 29–37.
 (26) Salzmann, C. G.; Llewellyn, S. A.; Tobias, G.; Ward, M. A. H.; Huh, Y.; Green, M. L. H. *Adv. Mater.* **2007**, *19*, 883–887.
 (27) Shao, L.; Tobias, G.; Salzmann, C. G.; Ballesteros, B.; Hong, S. Y.; Crossley, A.; Davis, B. J.; Green, M. L. H. *Chem. Commun.* **2007**, 5090–5092.
 (28) Price, B. K.; Lomeda, J. R.; Tour, J. M. *Chem. Mater.* **2009**, *21*, 3917–3923.
 (29) Worsley, K. A.; Kalinina, I.; Bekyarova, E.; Haddon, R. C. *J. Am. Chem. Soc.* **2009**, *131*, 18153–18158.
 (30) Chen, J.; Hamon, M. A.; Hu, H.; Chen, Y.; Rao, A. M.; Eklund, P. C.; Haddon, R. C. *Science* **1998**, *282*, 95–98.
 (31) Hamon, M. A.; Chen, J.; Hu, H.; Chen, Y. S.; Itkis, M. E.; Rao, A. M.; Eklund, P. C.; Haddon, R. C. *Adv. Mater.* **1999**, *11*, 834–840.
 (32) Kahn, M. G. C.; Banerjee, S.; Wong, S. S. *Nano Lett.* **2002**, *2*, 1215–1218.
 (33) Hu, H.; Zhao, B.; Hamon, M. A.; Kamaras, K.; Itkis, M. E.; Haddon, R. C. *J. Am. Chem. Soc.* **2003**, *125*, 14893–14900.

- (34) Kostarelos, K.; Lacerda, L.; Pastorin, G.; Wu, W.; Wieckowski, S.; Luangsilavilay, J.; Godefroy, S.; Pantarotto, D.; Briand, J. P.; Muller, S.; Prato, M.; Bianco, A. *Nat. Nanotechnol.* **2007**, *2*, 108–113.
 (35) Bonifazi, D.; Nacci, C.; Marega, R.; Campidelli, S.; Ceballos, G.; Modesti, S.; Meneghetti, M.; Prato, M. *Nano Lett.* **2006**, *6*, 1408–1414.
 (36) Bergeret, C.; Cousseau, J.; Fernandez, V.; Mevellec, J. Y.; Lefrant, S. *J. Phys. Chem. C* **2008**, *112*, 16411–16416.
 (37) Movia, D.; Del Canto, E.; Giordani, S. *J. Phys. Chem. C* **2010**, *114*, 18407–18413.
 (38) Del Canto, E.; Flavin, K.; Natali, M.; Perova, T.; Giordani, S. *Carbon* **2010**, *48*, 2815–2824.
 (39) Liu, J.; Rinzler, A. G.; Dai, H.; Hafner, J. H.; Bradley, R. K.; Boul, P. J.; Lu, A.; Iverson, T.; Shelimov, K.; Huffman, C. B.; Rodriguez-Macias, F.; Shon, Y. S.; Lee, T. R.; Colbert, D. T.; Smalley, R. E. *Science* **1998**, *280*, 1253–1256.
 (40) Ziegler, K. J.; Gu, Z. N.; Peng, H. Q.; Flor, E. L.; Hauge, R. H.; Smalley, R. E. *J. Am. Chem. Soc.* **2005**, *127*, 1541–1547.

Scheme 1. Representation of Purification and Oxidation of SWNTs^a



^a(A) HNO₃ 2.6 M, 100 °C, 48 h; (B) NaOH 8M, 100 °C, 48 h in triplicate; (C) neutralization with HCl and concentration to a solid; (D, E) H₂SO₄/H₂O₂ 4:1, 35 °C, 1 h; (F) NaOH 8M, 100 °C, 48 h.

The introduction and removal of specific functional groups, following each treatment was monitored by infrared spectroscopy. The appearance of absorption bands related to carbonyl stretching (1724 cm⁻¹) and the stretching of C=C bonds in the polyaromatic backbone of the tubes (1570–1580 cm⁻¹),^{29,41} are clearly evident following treatment with nitric acid (Figure 1A). The carbonyl stretching vibration may be assigned to carboxylic acid groups (COOH) produced either at defect sites on the nanotubes or on other carbonaceous material in the sample. This band notably decreased after NaOH treatment (Figure 1B), indicating that COOH functionalities in the sample were mainly present on the carbonaceous fragments which could be washed away after conversion to the more soluble sodium salt (Figure S1, Supporting Information). Analysis of the filtrate demonstrated the presence of CCFs in accordance with the literature (Scheme S1, Supporting Information).⁴²

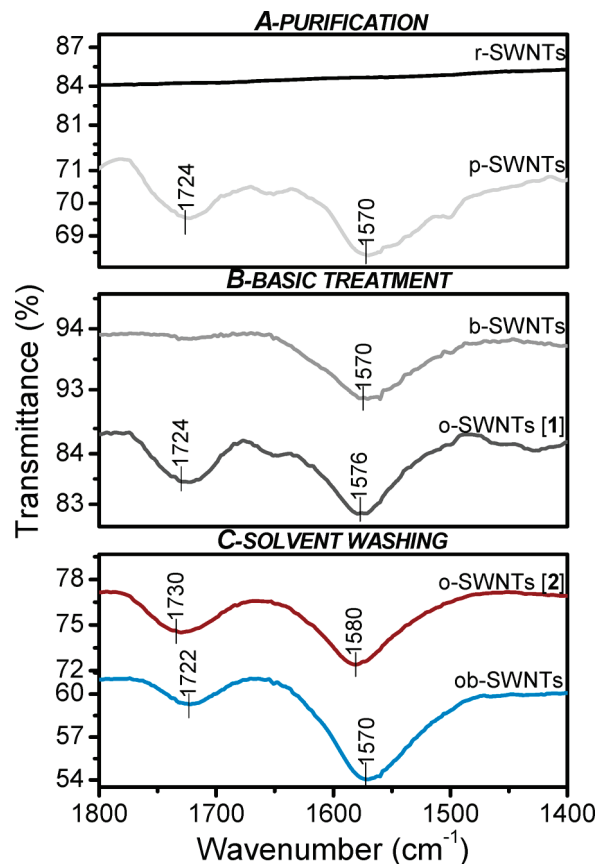


Figure 1. ATR/FT-IR spectra of (A) raw (r-SWNTs) and purified (p-SWNTs), (B) base-treated (b-SWNTs) and oxidized (o-SWNTs 1), and (C) oxidized (o-SWNTs 2) and oxidized base-treated (ob-SWNTs) nanotubes, where spectra have been baseline corrected to improve data visualization.

Following oxidation to o-SWNTs 1, the carbonyl stretching vibration is seen to reappear. As infrared spectroscopy cannot distinguish between COOH groups attached to the nanotubes and those attached to carbonaceous material, o-SWNTs 1 and 2 appear almost identical (Figure 1B and C). A small portion of o-SWNTs 2 was treated with base to investigate the presence of CCFs, following the solvent washing procedure. Only a small reduction in the carbonyl band is observed going from o-SWNTs 2 to oxidized base-washed nanotubes ob-SWNTs (Figure 1C), strongly indicating that the COOH functionalities present in the sample are indeed on the SWNTs. The filtrates from both NaOH treatments are illustrated in Figure 2, and the difference in the quantity of CCFs washed from each sample is evident from the filtrate color, demonstrating the influence of the solvent washing and the oxidation procedure on the composition of the sample.

Raman spectroscopy was used to monitor the introduction of defects into each sample, by monitoring changes in the intensity ratio of the characteristic D- (defect) and G- (graphitic) bands (Figure 3).^{43,44} Following the purification procedure the I_D/I_G ratio increased from 14 to 44% indicating breakage of the graphene sheet

(41) Tobias, G.; Shao, L.; Ballesteros, B.; Green, M. L. H. *J. Nanosci. Nanotechnol.* **2009**, *9*, 6072–6077.

(42) Fogden, S.; Verdejo, R.; Cottam, B.; Shaffer, M. *Chem. Phys. Lett.* **2008**, *460*, 162–167.

(43) Lazzeri, M.; Piscanec, S.; Mauri, F.; Ferrari, A. C.; Robertson, J. *Phys. Rev. B* **2006**, *73*, 155426.

(44) Graupner, R. *J. Raman Spectrosc.* **2007**, *38*, 673–683.



Figure 2. Pictures of the filtrates following NaOH treatments of (A) p-SWNTs and (B) o-SWNTs 2.

symmetry (Figure 3A). In this case the symmetry disruption is associated with the introduction of defects on both the nanotubes and the carbonaceous fragments. The relative intensity of the D-band subsequently decreased from 44 to 21% following NaOH treatment, in accordance with literature values (Figure 3B).^{26,29,42} The persistence of amorphous carbon (not containing acidic functionality) in the sample is however clear from the magnitude and shape of the D-band. The relative intensity again increased to 26% following the oxidation to o-SWNTs 1, indicating the introduction of defects on both the nanotubes and amorphous carbon (Figure 3B).

When compared to o-SWNTs 2, where the sample was washed with NMP instead of aqueous base, the relative D-band intensity dropped to below that of the raw material (Figure 3C). This coupled with the restored sharpness and symmetry of the band, strongly indicates that the oxidation step in combination with the NMP treatment results in removal of both the CCFs and amorphous carbon from the sample. The NaOH treatment of o-SWNTs 2 confirms this, demonstrating only a small reduction of the I_D/I_G ratio (Figure 3C). Enlarged spectra, shown in Figure S2, Supporting Information, clearly contrast the broad unsymmetrical D-band of o-SWNTs 1 with the sharper more symmetrical D-band of o-SWNTs 2.

X-ray photoelectron spectroscopy (XPS) was used to evaluate the changes in the chemical nature of the functional groups present in the sample by the different steps of the purification/oxidation process. Figure 4 illustrates the C 1s and O 1s core level spectra for each sample in addition to the fitting into the various components used to reproduce the spectra.

Characteristic contributions including the primary graphitic peak (284.4 eV) and plasmon loss (290.6 eV) are evident from the C 1s peak of the r-SWNTs. Following nitric acid purification a number of new contributions

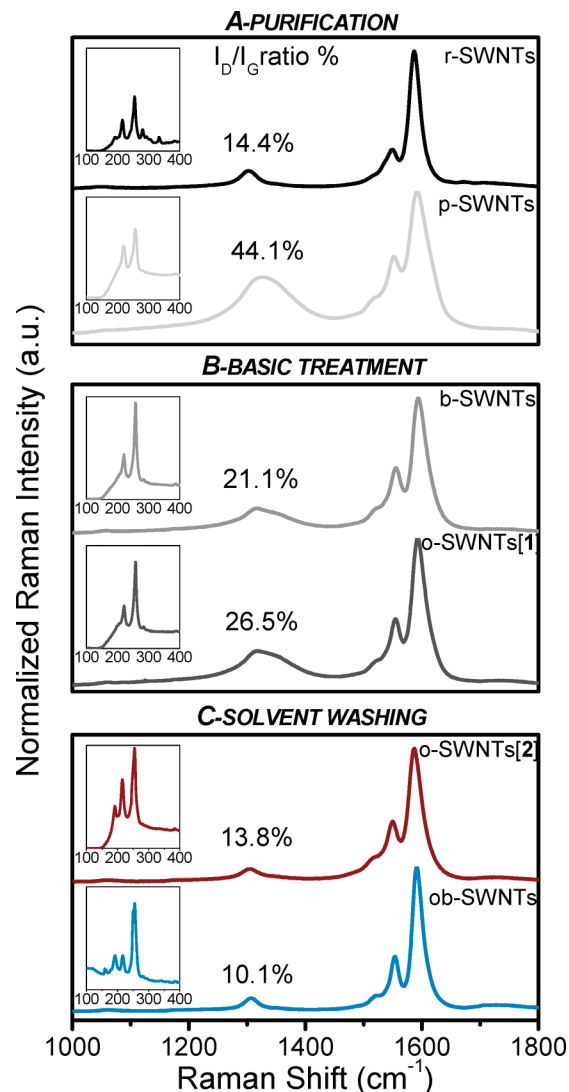


Figure 3. Raman spectra ($\lambda_{exc}=633$ nm) of (A) r-SWNTs and p-SWNTs, (B) b-SWNTs and o-SWNTs 1, and (C) o-SWNTs 2 and ob-SWNTs. All the spectra have been normalized on the G-band. Insets show the RB bands (scale = 0–0.24 au).

appear, which can be associated to the increasing sp^3 content (285.3 eV)⁴⁶ and the grafting of oxygen containing functionality (286–289 eV) onto the sample, most notably carboxylic acid groups at 288.8 eV.⁴⁷ Following NaOH treatment a reduction in the intensity of both the sp^3 and carboxylic acid components is observed indicating removal of CCFs, while after oxidation to o-SWNTs 1, as expected, the intensity of the component associated to carboxylic acid increases. When o-SWNTs 1 and 2 are compared the C 1s peak and its components appear much the same, indicating the similarity in the type and quantity of functionality present whether or not NaOH treatment is performed.

Analysis of the O 1s peak reveals the presence of iron oxide catalyst (530 eV)⁴⁸ in the raw material, which disappears following the purification procedure. A 4-fold

(46) Estrade-Szwarckopf, H. *Carbon* **2004**, *42*, 1713–1721.

(47) Jung, A.; Graupner, R.; Ley, L.; Hirsch, A. *Phys. Status Solidi B* **2006**, *243*, 3217–3220.

(48) Datsyuk, V.; Kalyva, M.; Papagelis, K.; Parthenios, J.; Tasis, D.; Siokou, A.; Kallitsis, I.; Galiotis, C. *Carbon* **2008**, *46*, 833–840.

(45) Giordano, R.; Serp, P.; Kalck, P.; Kihn, Y.; Schreiber, J.; Marhic, C.; Duvail, J.-L. *Eur. J. Inorg. Chem.* **2003**, *2003*, 610–617.

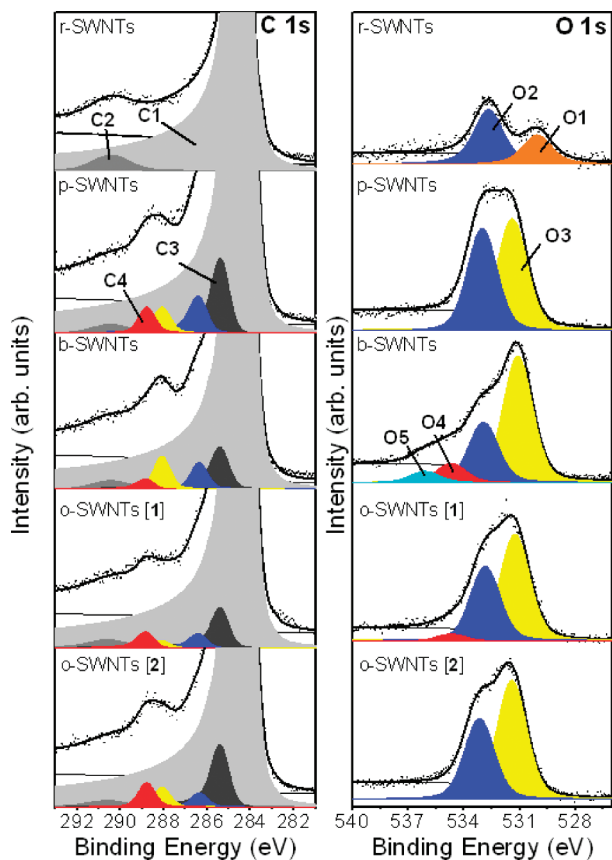


Figure 4. XPS C 1s and O 1s spectra of r-SWNTs, p-SWNTs, b-SWNTs, o-SWNTs 1, and o-SWNTs 2, where fitted components are labeled as C1, C–C sp²; C2, plasmon loss; C3, C–C sp³; C4, (C=O)–O–; O1, Fe₂O₃/Fe₃O₄; O2, C–O–C/(C=O)–O–/C–OH; O3, (C=O); O4, (C=O)–O–Na;⁴⁵ O5, H₂O.

increase in the oxygen content of the sample also occurs as expected, which is accompanied by the appearance of an additional component at 531.3 eV representing oxygen species of lower binding energy.⁴⁷ Following NaOH treatment a reduction in the relative intensity of the carboxylic acid containing component is evident, presumably because of the removal of CCFs. In accordance with the IR and Raman results this contribution again increases following the oxidation procedure indicating introduction of carboxylic acid functionality onto the SWNTs. On comparison of o-SWNTs 1 and 2, it is again evident that the oxygen containing functionality in each sample is similar both in the presence or absence of NaOH treatment.

To fully exploit the remarkable properties of SWNTs, the preservation of optical and electronic properties following chemical treatments is an important factor.^{6,16,17} The effect of each treatment on the structured emission and absorption features of the SWNTs was monitored by NIR-PL and UV–vis/NIR absorption spectroscopies, and the results are illustrated in Figures 5 and 6, respectively. The NIR-PL spectra clearly show that all nanotubes samples display a structured emission in the NIR (Figure 5 and Figure S3, Supporting Information), and in addition, UV–vis/NIR absorption data demonstrate the persistence of the van Hove singularities (Figure 6), which is in accordance with our previously reported results.³⁷

The assignment of the optical frequencies demonstrate that the bands at smaller wavelengths (900–1050 nm), corresponding to small diameter SWNTs, are completely destroyed during the purification procedure. This is in agreement with the loss of smaller diameter bands from the RBM region of the Raman spectra (Figure 3). The complete destruction of these SWNTs implies that all nanotubes in the sample have been affected by the acidic treatment and indicates that the PL observed is not simply because of the presence of unaltered nanotubes.

The investigation into quenching of the NIR-PL, following each chemical treatment (Figure 5D), has also given us a useful insight into the extent of defect introduction on the SWNTs with minimal interference from the other carbonaceous impurities present in the sample. The average NIR emission efficiency was evaluated for all SWNT samples (Figure 5D), and it is clear that a 90% quenching of the photoluminescence was observed following the purification procedure (see NIR-PL efficiency calculations in the Supporting Information). Under acidic conditions, this is known to occur as a result of protonation reactions at the nanotube surface.^{49–51} However, Weisman and co-workers have demonstrated that this doping process is completely reversible upon addition of base.^{50,51} Following NaOH treatment of the p-SWNTs, reappearance of the PL is observed, but only to 30% of the original intensity, demonstrated by the raw material. We thus propose that the irreversible quenching observed, originates from defects produced in the nanotube structure during the purification procedure, as opposed to reversible doping by protonation. If we also consider that functionality introduced onto the nanotube structure during the purification procedure, for a large extent, does not seem to consist of carbonyl containing moieties (Figure 1B), the highly oxidative treatment seems necessary, to convert the defects into reactive COOH groups.

Following the oxidation procedure the NIR-PL of o-SWNTs 1 and 2 again drops to a value of approximately 10%, which is most probably the result of both defect introduction and doping processes. After NaOH treatment of o-SWNTs 2, an increase in the PL efficiency is evident; however, it is still smaller than b-SWNTs suggesting the introduction of additional defects during the oxidation step.

TGAs were performed on each sample in air, and following treatment with nitric acid, nearly quantitative removal of the catalyst was demonstrated, where the residual ash content at 900 °C dropped from 34% in the raw material to 1% (Figure S5 and Table S1, Supporting Information). This was confirmed by HR-TEM (Figure S6, Supporting Information), where the high content of iron

(49) Cagnet, L.; Tsyboulski, D. A.; Rocha, J. D. R.; Doyle, C. D.; Tour, J. M.; Weisman, R. B. *Science* **2007**, *316*, 1465–1468.

(50) O’Connell, M. J.; Bachilo, S. M.; Huffman, C. B.; Moore, V. C.; Strano, M. S.; Haroz, E. H.; Rialon, K. L.; Boul, P. J.; Noon, W. H.; Kittrell, C.; Ma, J.; Hauge, R. H.; Weisman, R. B.; Smalley, R. E. *Science* **2002**, *297*, 593–596.

(51) Strano, M. S.; Huffman, C. B.; Moore, V. C.; O’Connell, M. J.; Haroz, E. H.; Hubbard, J.; Miller, M.; Rialon, K.; Kittrell, C.; Ramesh, S.; Hauge, R. H.; Smalley, R. E. *J. Phys. Chem. B* **2003**, *107*, 6979–6985.

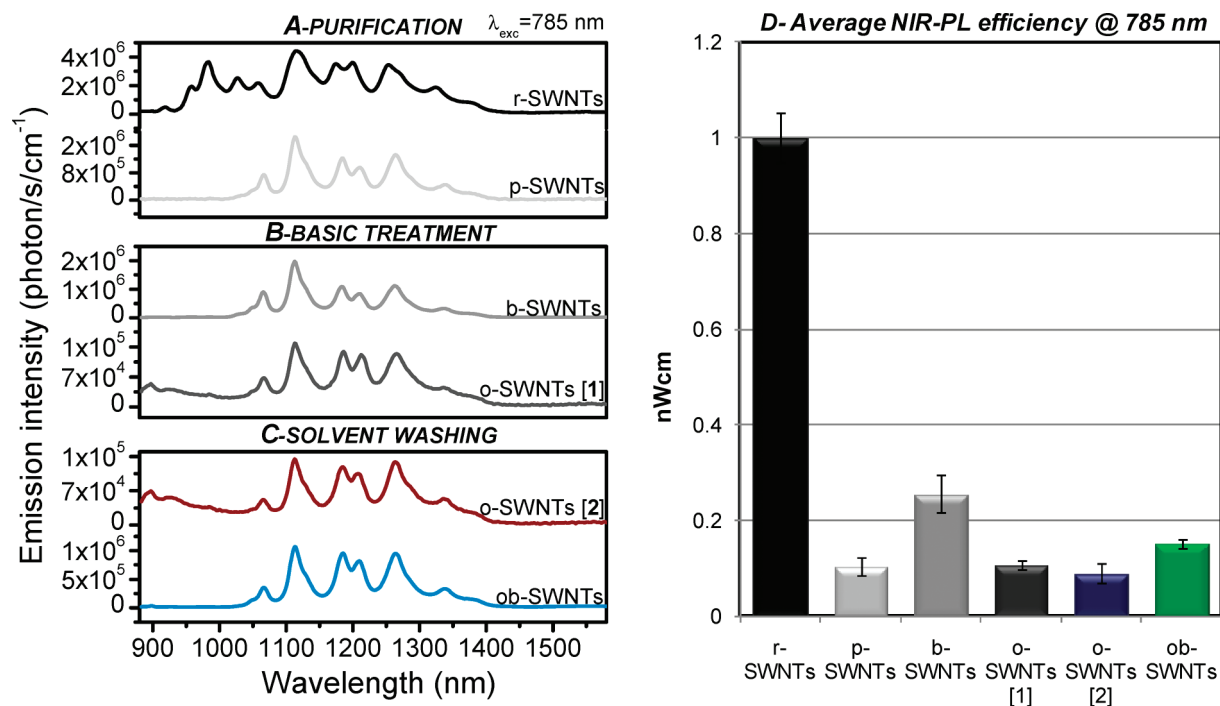


Figure 5. NIR photoluminescence (PL) spectra ($\lambda_{exc} = 785$ nm) of (A) r-SWNTs and p-SWNTs, (B) b-SWNTs and o-SWNTs 1, and (C) o-SWNTs 2 and ob-SWNTs. (D) Histograms showing the average NIR-PL efficiency at $\lambda_{exc} = 785$ nm ($n_{\text{measurements}} = 3$).

catalyst, visible as black particles in the r-SWNTs, is absent in the purified material. TGAs were also performed under a nitrogen atmosphere (Figure S7 and Table S2, Supporting Information). On comparison of both the curve shape and the weight loss below 400 °C, before and after treatment with NaOH, a significant change is observable which is indicative of the effectiveness of the NaOH treatment in the removal of carbonaceous material from the p-SWNTs.

AFM topographic images of r-SWNTs, p-SWNTs, and b-SWNTs displayed the effectiveness of purification and washing protocols in progressively removing catalyst and carbonaceous impurities going from r-SWNTs to b-SWNTs (Figure S8, Supporting Information). Additionally, AFM images of o-SWNTs 1 and 2 confirmed the shortening of the tubes after oxidation treatments, where average lengths were estimated at 482 ± 170 and 528 ± 159 nm, respectively (Figure S9, Supporting Information).

Functionalization. A fluorescent probe, fluoresceinamine, was coupled to both o-SWNTs 1 and 2, as illustrated in Scheme 2, to investigate the presence of COOH functional groups on o-SWNTs 1 and 2.

To remove the excess of nonreacted reagents from f-SWNTs 1 and 2, the samples were dispersed in DMF by sonication and washed with a number of solvents until the filtrate ran clear. The fluorescent probe, although not concentrated enough to be seen using UV-vis/NIR absorption spectroscopy (Figure S10, Supporting Information), is clearly observable from the emission spectra of both f-SWNT samples excited at 490 nm (Figure 7

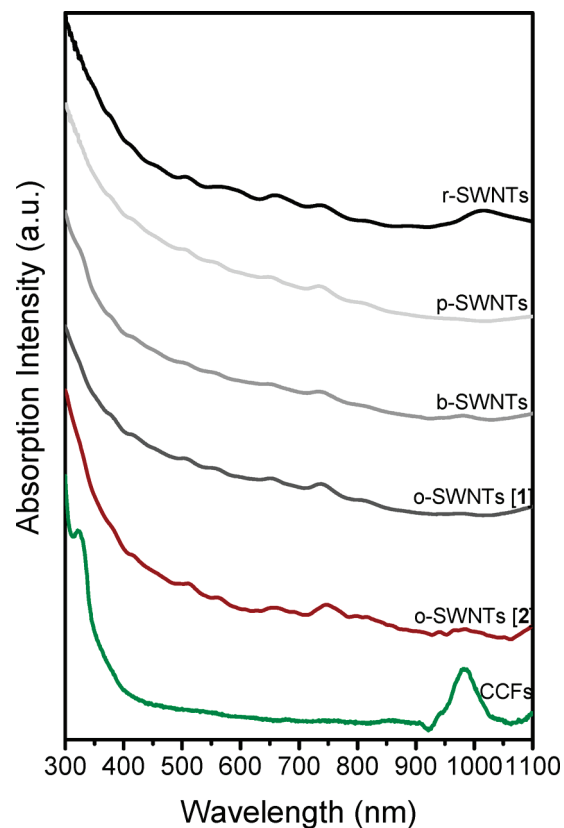


Figure 6. UV-vis/NIR absorption profiles of all samples in DMF. Absorption values (y-axes) have been varied to better visualize the van Hove singularities. Spectra with actual absorption intensity values are reported in Figure S4, Supporting Information.

and Supporting Information Figure S11).⁵² To compare the samples at similar concentrations, they were diluted until equal values of optical absorption were observed

(52) Nakayama-Ratchford, N.; Bangsaruntip, S.; Sun, X.; Welsher, K.; Dai, H. *J. Am. Chem. Soc.* **2007**, *129*, 2448–2449.

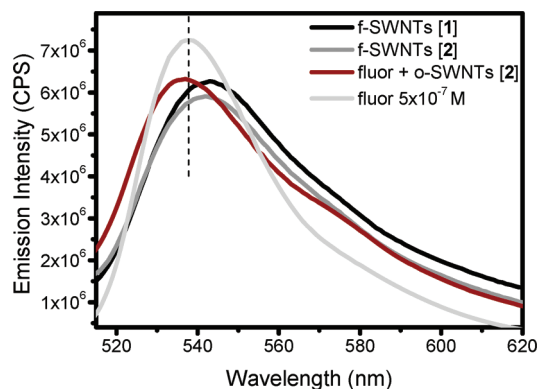
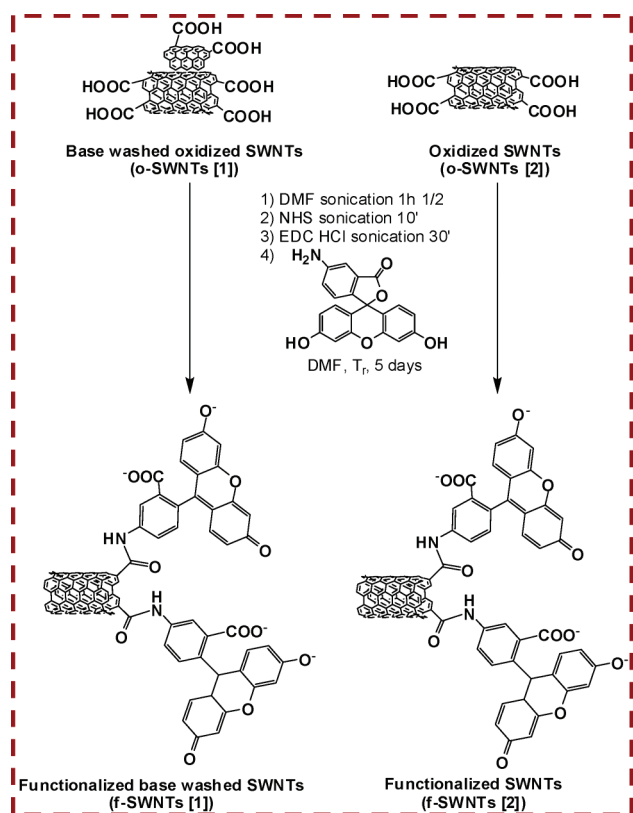


Figure 7. Emission profiles ($\lambda_{\text{exc}}=490$ nm) of fluoresceinamine, f-SWNTs **1** and **2**, and fluoresceinamine π - π stacked to o-SWNTs **2**. The nanotube samples have been diluted until same optical absorption values in DMF.

Scheme 2. Coupling Reaction of Oxidized SWNTs **1 and **2** with Fluoresceinamine**



(Figure S10, Supporting Information). Following excitation of these solutions the emission intensities suggest that the degree of functionalization of both samples is comparable, affording similarly functionalized materials. When compared to the fluorescent probe alone in DMF, a red-shift in the maximum emission intensity is observed from 538 to 545 nm for both the f-SWNT **1** and **2**. To investigate whether the red-shift originates from covalent attachment or from noncovalent interaction, fluoresceinamine was titrated into a solution of o-SWNTs **2**. This resulted in a slight blue-shift of the emission maximum to 536 nm, strongly indicating that the fluorescent probe is covalently bound to the SWNT structure in the functionalized samples and not simply

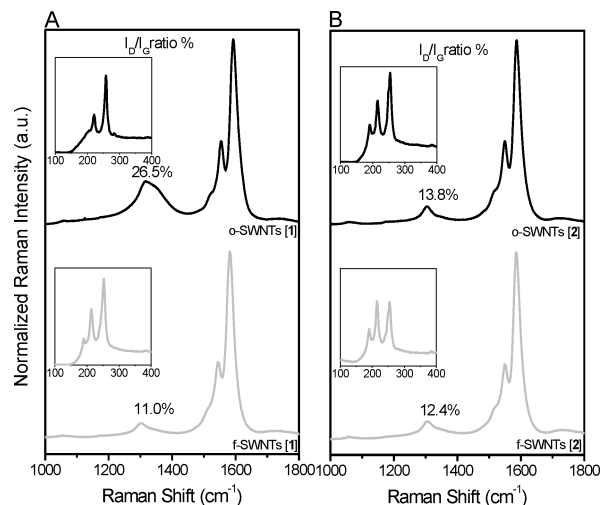


Figure 8. Raman spectra ($\lambda_{\text{exc}} = 633$ nm) of (A) o-SWNTs **1** and f-SWNTs **1** and (B) o-SWNTs **2** and f-SWNTs **2** normalized on the G-band. Insets show the RBM bands (scale = 0–0.25 au).

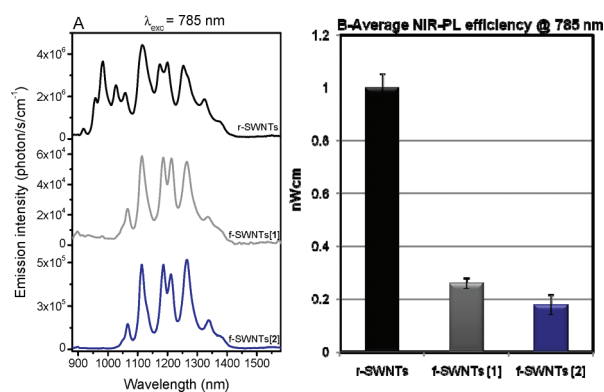


Figure 9. (A) NIR-PL spectra ($\lambda_{\text{exc}} = 785$ nm) of r-SWNTs, f-SWNTs **1**, and f-SWNTs **2**. (B) Histograms showing the average NIR-PL efficiency at $\lambda_{\text{exc}} = 785$ nm ($n_{\text{measurements}} = 3$).

physisorbed to the surface as previously seen by Dai and co-workers.⁵²

The Raman spectra of both batches of the oxidized and functionalized SWNTs are illustrated in Figure 8, and interestingly, a decrease of the $I_{\text{D}}/I_{\text{G}}$ ratio is observed for both following functionalization. Although the decrease is practically negligible in the case of f-SWNTs **2**, a quite substantial drop is evident for f-SWNTs **1**, which seem to occur because of the removal of the remaining carbonaceous material from the sample by solvent washing.

NIR-PL spectra of the functionalized samples are illustrated in Figure 9 (and Figure S12, Supporting Information), and it is evident that structured emission is sustained, indicating retention of the characteristic optical/electronic properties following covalent functionalization. The removal of the remaining carbonaceous material from the oxidized samples, following solvent washing, is also evident from the reduction in emission in the 880–1000 nm region of the spectrum.

Representative AFM topographic images of single f-SWNTs **1** and **2** with the height profiles are reported in the Supporting Information (Figure S13).

Conclusions

Using a well-known 2-step purification/oxidation procedure, in the absence of NaOH treatment, we have demonstrated that COOH functionality is introduced directly onto SWNTs and not only onto carbonaceous material present in the sample, as previously reported for single step nitric acid purification. FT-IR, Raman, NIR-PL, and XPS were used to demonstrate that both solvent washing and oxidation procedures are important with regards to the removal of carbonaceous material and conversion of introduced defects to reactive COOH groups, respectively. Covalent functionalization of the oxidized materials was also investigated by attachment of a fluorescent probe, and ultimately, whether treated with base- or solvent-washed, the resulting materials are close to identical with respect to both their appearance and properties. In addition, we have demonstrated that using either of these purification/oxidation strategies, functionalized materials can be produced that still exhibit their distinctive optical/electronic properties, as demonstrated by sustained structured spectroscopic absorption and emission features.

Acknowledgment. This work was supported by Science Foundation Ireland (PIYRA 07/YI2/I1052). The authors wish to thank the support of IRCSET and Intel (Postgraduate Research Scholarships to E.D.C. and M.D.) and Dr. Tatiana Perova for help and support with Raman spectroscopy.

Supporting Information Available: Experimental section including, general methods, NIR-PL efficiency calculations, experimental procedures, and additional schemes and figures, including, detailed solvent washing procedures and filtrates pictures, FT-IR and Raman spectra of CCFs, Raman spectra of oxidized SWNTs **1** and SWNTs **2**, NIR PL spectra of all the nanotubes samples and CCFs at $\lambda_{\text{exc}} = 638$ nm and $\lambda_{\text{exc}} = 683$ nm, UV-vis/NIR absorption spectra of all the nanotubes samples and CCFs with actual absorption intensity values, TGA traces of r-SWNTs and p-SWNTs, weight loss at 310 °C of all the nanotubes samples and CCFs, HR-TEM of all the nanotubes samples and CCFs, AFM topographic images of r-SWNTs, p-SWNTs, b-SWNTs, o-SWNTs **1** and **2**, and emission profiles of all the nanotubes samples and CCFs. This material is available free of charge via the Internet at <http://pubs.acs.org>.